The Hydrogen Peroxide−Rare Gas Systems: Quantum Chemical Calculations and Hyperspherical Harmonic Representation of the Potential Energy Surface for Atom−Floppy Molecule Interactions†

Patricia R. P. Barreto,‡ Alessandra F. A. Vilela,§ Andrea Lombardi,# Glauciete S. Maciel,# Federico Palazzetti,*,# and Vincenzo Aquilanti#

Laboratório Associado de Plasma (LAP), Instituto Nacional de Pesquisas Espaciais (INPE)/MCT, CP 515, São José dos Campos, São Paulo, CEP 1224 7-9 70, Brazil, Instituto de Física, Universidade de Brasília, Brasília, DF, CEP 70919-970, Brazil, and Dipartimento di Chimica, Universitá di Perugia, 06100 Perugia, Italy

Received: August 5, 2007; In Final Form: October 11, 2007

A quantum chemical exploration is reported on the interaction potentials of H_2O_2 with the rare gases, He, Ne, Ar, Kr, and Xe. Hydrogen peroxide (the simplest example of chiral molecule in its equilibrium geometry) is modeled as rigid except for the torsional mode around the O−O bond. However, on the basis of previous work (Maciel, G. S.; et al. *Chem. Phys. Lett.* **2006** *432,* 383), the internal mode description is based, rather than on the vectors of the usual valence picture, on the orthogonal local representation, which was demonstrated useful for molecular dynamics simulations, because the torsion around the vector joining the center-of-mass of the two OH radicals mimics accurately the adiabatic reaction path for chirality changing isomerization, following the torsional potential energy profile from equilibrium through the barriers for the *trans* and *cis* geometries. The basic motivation of this work is the determination of potential energy surfaces for the interactions to be used in classical and quantum simulations of molecular collisions, specifically those leading to chirality changes of possible relevance in the modeling of prebiotic phenomena. Particular attention is devoted to the definition of coordinates and expansion formulas for the potentials, allowing for a faithful representation of geometrical and symmetry properties of these systems, prototypical of the interaction of an atom with a floppy molecule.

1. Introduction

We start this account of an investigation of the interactions of H_2O_2 with the rare gases by listing a few motivations. Stimulated in part by the interesting problem of large amplitude vibrations, such as the chirality change transitions associated with the torsional motions around the O−O and S−S bonds, a systematic series of quantum chemical studies has been undertaken on systems that play roles in biological and combustion chemistry, and in particular in the photochemistry of the minor components of the atmosphere,[1] specifically hydrogen peroxide.[2] Further studies regarded several systems obtained by substitutions of the hydrogens in H_2O_2 by alkyl groups,[3] halogens,[4] and the analogous H_2S_2 and disulfanes.[5] Quantum chemistry has been proved to have reached the stage of resolving many previously controversial features for these series of molecules (dipole moment, equilibrium geometries, heights of barriers for the chirality changing mode), which are crucial for intramolecular dynamics, and quantum dynamics calculations have also been performed to compute torsional levels and the temperature dependence of their distributions. For intermolecular interactions of H_2O_2 with various molecules and ions see also refs 6−8, and with itself see ref 9 and references therein.

In this laboratory, previous joint experimental and theoretical studies have been devoted to interactions of H_2O with rare gases,[10] for which state-of-the-art quantum chemical calculations have yielded complementary information on the interactions (specifically the anisotropies) with respect to molecular beam scattering experiments that measure essentially the isotropic forces.[10] Similar approaches and results have been pursued and obtained for the H_2S−rare gas systems.[11] The experiments probe intermolecular interactions by scattering measurements.[12] Interesting alignment and orientation effects in the gas phase were experimentally demonstrated, as due to molecular collisions, and occurring typically when in a gaseous mixture a "heavier" molecular component is seeded in a lighter one. The detection of aligned oxygen in gaseous streams[13] and further evidence on simple molecules have been extended to benzene and various hydrocarbons; see refs 14 and 15 and references therein. Other investigations suggest that chiral effects can be seen in the differential scattering of oriented molecules, in particular from surfaces: this is reviewed in a previous paper,[16] where it is further pointed out that a possible mechanism of chiral biostereochemistry of oriented reactants, acting through selective collisions, may be of prebiotical interest.[16,17] The dynamical treatment of such collisions requires information on the nature and mechanical properties of the peroxidic bond and the associated torsional motion.

In the present paper we investigate the interaction of hydrogen peroxide with the rare gases. These systems involve five atoms, but the intramolecular modes of the hydrogen peroxide are considered to be frozen except for the torsional angle γ (see Figure 1 and ref 2). It is shown that the interaction potential for this atom−floppy molecule problem can be expressed as a

† Part of the "Giacinto Scoles Festschrift".

* Corresponding author. E-mail: fede@dyn.unipg.it.
‡ Instituto Nacional de Pesquisas Espaciais.
§ Universidade de Brasília.
# Universitá di Perugia.

10.1021/jp076268v CCC: $37.00
Published on Web 11/14/2007

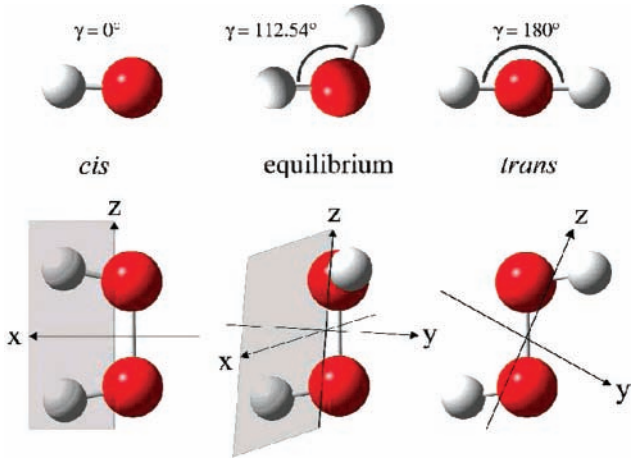

Figure 1. Hydrogen peroxide illustrated in three characteristic molecular geometries: the two planar *cis* (closed book) and *trans* (open book), and the equilibrium one. The angle measuring the torsion around the −O−O− bond (the opening of the book), is denoted as γ, the dihedral angle H−O−O−H. In the upper side of the figure we have views of the molecule alongside the O−O bond. The lower panels show the coordinate frame used in this paper. In all three cases, three of the atoms (the lower hydrogen and the two oxygens) lie in the plane of the drawing. The origin is taken in the instantaneous center-of-mass of the molecule. The *z* axis of the right-handed Cartesian frame is taken alongside the Jacobi vector, which joins the centers-of-mass of the two OH vectors. The *xz* plane lies in the plane of the drawing for the *cis* geometry, and perpendicular to the plane of the drawing in the *trans* case. It moves bisecting symmetrically the spine of the book as it opens. In the *cis* and *trans* cases, the *y* and *x* axes are perpendicular to the plane of the drawing and point toward the reader.

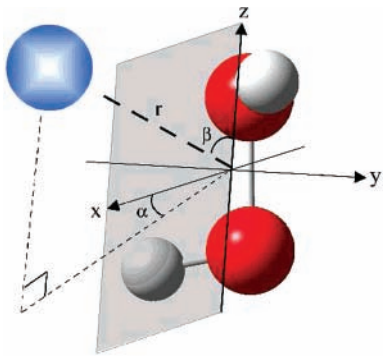

Figure 2. Definition of the spherical coordinates of the vector $\vec{r} = r$, β, α specifying the position of the rare gas atom in the reference frame of Figure 1. *r*, β, and α coordinates are illustrated for the case of the equilibrium geometry (see Figure 1). *r* is the distance between the center-of-mass of the molecule and the rare gas atom, β is the angle between $\vec{r}$ and the *z* axis, and α is the angle between the *x* axis and the projection of $\vec{r}$ onto the *xy* plane.

function of four variables: the polar coordinates *r*, α, and β (see Figure 2) and the dihedral angle γ. Because the range of angular variables spans a three-dimensional manifold isomorphic to S^3 (the sphere embedded in the four dimensional Euclidean space $\mathscr{R}^4$), the proper orthonormal expansion basis set is in terms of hyperspherical harmonics (see, for example, refs 18 and 19). We define such a basis set in terms of real combinations of Wigner D-functions, which are described and tabulated, for example, in ref 20.

To determine the expansion moments for the hyperspherical expansion, we use a dozen "significant" configurations (at fixed α, β, and γ) whose potential energy profiles as a function of *r* are calculated by state-of-the-art *ab initio* techniques.

The plan of the paper is as follows. In section 2 we discuss the representation of the potential energy surfaces, considering in section 2.1 coordinates and symmetries and in section 2.2 an expansion of the potential interaction in terms of hyperspherical harmonics built as linear combinations of Wigner D-functions to obtain real hyperspherical harmonics. Section 2.3 describes specific configurations that we considered representative of the full potential energy surfaces. We call them "leading configurations" and obtain explicitly their connections with the moments of the hyperspherical harmonics expansion. In section 3 the *ab initio* calculations for such configurations are presented, and in section 4 we discuss the results. Conclusions follow in section 5.

2. Representation of the Potential Energy Surfaces

2.1. Coordinates and Symmetries. The positions of the rare gas atom with respect to the H_2O_2 molecule is expressed in terms of the spherical polar coordinates $\vec{r} = (r, \alpha, \beta)$, where α and β are the azimuthal and polar angle, respectively (Figure 2). The origin is the instantaneous center-of-mass of the H_2O_2 molecule (it coincides with the middle of the O−O bond for the *trans* geometry). In ref 2 we gave arguments that the internal torsional motion around the O−O bond is actually best described as a rotation of the two OH radicals around the Jacobi vector[21] joining their centers of mass, rather than as a rotation around the O−O bond axis. This is an example of the use of local orthogonal coordinates;[21] see also ref 22. Because in the case of the OH bond the center-of-mass is shifted with respect to the O position by only $\sim 1/17$th of the bond length, the Jacobi vector differs very little with respect to the O−O bond (see Figure 1 and 2). The *z* axis will be taken along the Jacobi vector. The corresponding torsional angle is denoted as γ ($0 \le \gamma < 2\pi$). The *xz* plane contains the Jacobi vector joining the two centers of mass and bisects symmetrically the instantaneous H_2O_2 molecular geometry, imagined as a "book", where the O−O bond (more precisely the Jacobi vector) is the spine. It coincides with the molecular plane in the planar geometries *cis* (closed book $\gamma = 0°$) and *trans* (fully open book $\gamma = 180°$). Angles α and β and distance *r* from the center-of-mass as the origin of the Cartesian reference frame are the spherical polar coordinates specifying the position of the rare gas atom:

$$x = r \sin\beta \cos\alpha$$
$$y = r \sin\beta \sin\alpha$$
$$z = r \cos\beta$$

($0 \le r \le \infty$, $0 \le \beta \le \pi$, $0 \le \alpha < 2\pi$), and the vector $\vec{r} = (r, \alpha, \beta)$ is itself a Jacobi vector, so that this representation will turn out to be particularly useful for dynamical treatments. It is seen that β is the angle between the positive *z* axis and the line formed between the atom position and the origin and α is the angle between the positive *x* axis and the projection of $\vec{r}$ onto the *xy* plane.

The potential describing the atom− floppy molecule systems depends on these four coordinates and can be easily checked to have the following symmetry properties:

$$V(r;\alpha,\beta,\gamma) = V(r;-\alpha,\beta,-\gamma) = V(r;-\alpha,\pi-\beta,\gamma) = V(r;\alpha,\pi-\beta,-\gamma) \quad (1)$$

The analytical form of the potential surface that will be built will have the property that *V* can be partitioned as a sum of two contributions as follows:

$$V(r;\alpha,\beta,\gamma) = V_{ext}(r;\alpha,\beta) + V_{int}(r;\gamma) \quad (2)$$

TABLE 1: Real Hyperspherical Harmonics $R^{\mu}_{MM'}(\alpha, \beta, \gamma)$ for $\mu = 1$

M/M'	1	0	−1
1	$[(1+\cos\beta)/\sqrt{2}](\cos\alpha\cos\gamma - \sin\alpha\sin\gamma)$	$-\sin\beta\cos\alpha$	$[(1-\cos\beta)/\sqrt{2}](\cos\alpha\sin\gamma - \sin\alpha\cos\gamma)$
0	$\sin\beta\cos\gamma$	$\cos\beta$	$-\sin\beta\sin\gamma$
−1	$[(1-\cos\beta)/\sqrt{2}](\cos\alpha\cos\gamma + \sin\alpha\sin\gamma)$	$\sin\alpha\sin\beta$	$[(1+\cos\beta)/\sqrt{2}](\sin\alpha\cos\gamma + \cos\alpha\sin\gamma)$

where the term $V_{ext}(r;\alpha,\beta)$ accounts for the interaction contribution depending on the atom−molecule relative distance r and orientation, and $V_{int}(r;\gamma)$ is the intramolecular atomic term depending on distance r and on the internal torsion dihedral angle γ.

2.2. Hyperspherical Harmonics Expansion. The manifold spanned by the angles α, β, and γ is isomorphic to the four dimensional hypersphere S^3 (see, e.g., refs 18 and 19). The potential energy function of eq 2 can be expanded into a series of appropriate angular functions multiplied by radial coefficients (expansion moments). A suitable complete orthonormal set is that of Wigner D-functions[23] (here in their role as hyperspherical harmonics), which depend on three Euler-like angles with the same domain as the spherical angles α and β and the torsion angle γ (see section 2.1).

The D-functions are in general complex, see, e.g., ref 20. Therefore we will work out an alternative orthonormal basis set imposing that the functions be real, denoting them as $R^{\mu}_{MM'}(\alpha,\beta,\gamma)$, in terms of which hyperspherical harmonics the expansion of the potential energy surface is as follows:

$$V(r;\alpha,\beta,\gamma) = \sum_{\mu,M,M'} v^{\mu}_{MM'}(r)\, R^{\mu}_{MM'}(\alpha,\beta,\gamma) \qquad (3)$$

where $\mu = 0, 1, 2, \ldots$ and M (M') $= -\mu, -\mu+1, \ldots, 0, 1, \ldots, \mu$ and the $v^{\mu}_{MM'}(r)$ coefficients are the expansion moments depending on the r coordinate. The truncation of the set of basis functions to a certain value of the index μ depends on the number of fixed atom−molecule configurations for which the potential energy is known as a function of r from *ab initio* calculations, as specified later on in the paper. In terms of the Wigner D-functions that are complex-valued, the $R^{\mu}_{MM'}(\alpha,\beta,\gamma)$ are found to be simple real-valued linear combinations:

$$R^{\mu}_{MM'}(\alpha,\beta,\gamma) = \sqrt{\frac{8\pi^2}{2(2\mu+1)}}(D^{\mu}_{MM'}(\alpha,\beta,\gamma) + \epsilon D^{\mu}_{-M-M'}(\alpha,\beta,\gamma)) \qquad (4)$$

$$R^{\mu}_{-M-M'}(\alpha,\beta,\gamma) = \mathrm{i}\sqrt{\frac{8\pi^2}{2(2\mu+1)}}(\epsilon D^{\mu}_{MM'}(\alpha,\beta,\gamma) - D^{\mu}_{-M-M'}(\alpha,\beta,\gamma)) \qquad (5)$$

where $\epsilon = (-1)^{M-M'}$.

Let us recall that $D^{\mu}_{MM'}(\alpha,\beta,\gamma) = \mathrm{e}^{\mathrm{i}m\alpha} d^{\mu}_{MM'}(\beta) \mathrm{e}^{\mathrm{i}M'\gamma}$, where the reduced Wigner rotation matrix elements $d^{\mu}_{MM'}(\beta)$ are connected to Jacobi polynomials in $\cos(\beta)$. In particular,

$$R^{\mu}_{00} = D^{\mu}_{00} = d^{\mu}_{00} \qquad (6)$$

essentially a Legendre polynomial in $\cos\beta$.

For $\mu = 0$, $R^{0}_{00}(\alpha,\beta,\gamma) = 1$. For $\mu = 1$ and $\mu = 2$ the basis sets of 34 functions that can be obtained are listed in Tables 1

TABLE 2: Real Hyperspherical Harmonics $R^{\mu}_{MM'}(\alpha,\beta,\gamma)$ for $\mu = 2$

M/M'	2	1	0	−1	−2
2	$[(1+\cos\beta)^2)/2\sqrt{2}](\cos 2\alpha\cos 2\gamma - \sin 2\alpha\sin 2\gamma)$	$[(\sin\beta(1+\cos\beta))/\sqrt{2}](\sin 2\alpha\sin\gamma - \cos 2\alpha\cos\gamma)$	$\sqrt{3}/2\sin^2\beta\cos 2\alpha$	$-[(\sin\beta(1-\cos\beta))/\sqrt{2}](\cos 2\alpha\cos\gamma - \sin 2\alpha\sin\gamma)$	$[((1-\cos\beta)^2)/2\sqrt{2}](\cos 2\alpha\sin 2\gamma - \sin 2\alpha\cos 2\gamma)$
1	$[(\sin\beta(1+\cos\beta))/\sqrt{2}](\cos\alpha\cos 2\gamma - \sin 2\alpha\sin\gamma)$	$[(2\cos^2\beta+\cos\beta-1)/\sqrt{2}](\cos\alpha\cos\gamma - \sin\alpha\sin\gamma)$	$-\sqrt{3}\sin\beta\cos\beta\cos\alpha$	$(2\cos^2\beta+\cos\beta-1)/\sqrt{2}(\cos\alpha\sin\gamma - \sin\alpha\cos\gamma)$	$[(\sin\beta(1-\cos\beta))/\sqrt{2}](\sin\alpha\cos 2\gamma - \cos\alpha\sin 2\gamma)$
0	$\sqrt{3}/2\sin^2\beta\cos 2\gamma$	$\sqrt{3}\sin\beta\cos\beta\cos\gamma$	$(3\cos^2\beta-1)/2$	$-\sqrt{3}\sin\beta\cos\beta\sin\gamma$	$(\sqrt{3}/2)\sin^2\beta\sin 2\gamma$
−1	$[(\sin\beta(1-\cos\beta)/\sqrt{2}](\cos\alpha\cos 2\gamma + \sin\alpha\sin 2\gamma)$	$[(2\cos^2\beta+\cos\beta-1)/\sqrt{2}](\cos\alpha\cos\gamma + \sin\alpha\sin\gamma)$	$\sqrt{3}\sin\beta\cos\beta\sin\alpha$	$[(2\cos^2\beta+\cos\beta-1)/\sqrt{2}](\sin\alpha\cos\gamma + \cos\alpha\sin\gamma)$	$[-(\sin\beta(1+\cos\beta)/\sqrt{2}](\sin\alpha\cos 2\gamma + \cos\alpha\sin 2\gamma)$
−2	$[((1-\cos\beta)^2)/2\sqrt{2}](\cos 2\alpha\cos 2\gamma + \sin 2\alpha\sin 2\gamma)$	$[(\sin\beta(1-\cos\beta))/\sqrt{2}](\sin 2\alpha\cos\gamma - \cos 2\alpha\sin\gamma)$	$\sqrt{3}/2\sin^2\beta\sin 2\alpha$	$[(\sin\beta(1+\cos\beta))/\sqrt{2}](\sin 2\alpha\cos\gamma - \cos 2\alpha\sin\gamma)$	$[((1+\cos\beta)^2)/2\sqrt{2}](\sin 2\alpha\cos 2\gamma + \cos 2\alpha\sin 2\gamma)$

TABLE 3: Definition of Leading Configurations, in Terms of the α, β, and γ Angles

		$\beta = 90°$			$\beta = 0°$
	γ [deg]	$\alpha = 0°$	$\alpha = 90°$	$\alpha = 180°$	α = ind
cis	0	$C_>$	$C_\perp$	$C_<$	$C_\parallel$
equilibrium	112.54	$E_>$	$E_\perp$	$E_<$	$E_\parallel$
trans	180	$T_>$	$T_\perp$	$T_<$	$T_\parallel$

and 2. Many of them can be excluded by enforcing the symmetry properties of the potential (eq 1), in such a way that all the functions depending on $\sin^n \alpha$, $\sin^n \gamma$, $\cos^n \beta$, where n is an integer odd number are discarded.

After the enforcing of the symmetry conditions, the basis set reduces to the six functions R^0_{00}, R^1_{10}, R^1_{01}, R^2_{00}, R^2_{20}, and R^2_{02}, whose corresponding coefficients in the expansion given in eq 3 will be the ones that will be provided in this work.

In general, use of properly selected potential energy profiles at fixed internal torsional angle γ and as a function of the distance r of the atom from the molecular center-of-mass, corresponding to approaches from different directions (specified by α and β) allows us to set up systems of linear equations (see eq 3), for the expansion moments $v^\mu_{MM'}(r)$. Therefore the solution for various r would give the moments that, inserted in eq 3, would provide the full potential energy surface. Our choice for specific configurations, corresponding to selected values of α, β and γ is described next.

2.3. Leading Configurations and Expansion Moments. The choice of the configurations relies upon physical considerations on the geometrical features of the systems. We considered three significant geometries of H_2O_2 corresponding to the equilibrium ($\gamma = 112.54°$), and to the *cis* and *trans* molecular geometry, with $\gamma = 0°$ and $\gamma = 180°$, respectively.[2] For each of these configurations the atom−molecule interaction has been calculated by considering the atom moving along the O−O bond direction ($\beta = 0°$ and α indetermined) and along the direction perpendicular to that bond ($\beta = 90°$), at $\alpha = 0°$, 90°, and 180°. These leading configurations are listed in Table 3. The expansion moments are then obtained as a linear combination of the potential profiles calculated for the above configurations. In the following section, we give details about the *ab initio* calculation of the potential profiles for the various leading configurations.

The representation of the potential energy as a sum of the intermolecular and intramolecular contributions (eq 2) can be obtained in terms of the real hyperspherical harmonics $R^\mu_{MM'}(\alpha,\beta,\gamma)$ by expanding the two terms (in eq 2) individually. The intramolecular term $V_{int}(r;\gamma)$ involves $R^\mu_{0M}(0,\Pi/2,\gamma)$ and $R^\mu_{0M}(0,0,\gamma)$ functions because it has to be independent from β and α. Conversely, the intermolecular term $V_{ext}(r;\alpha,\beta)$ only involves $R^\mu_{M0}(\alpha,\beta,0)$ basis functions. However, although not explicitly dependent on γ, $V_{ext}(r;\alpha,\beta)$ is referred to the three main H_2O_2 geometries (the *cis*, *trans*, and equilibrium geometry) and depends parametrically on γ.

The moments $v^\mu_{MM'}(i;r)$ (where the dependence upon the molecular geometry is now specified by the symbol $i = C$, E, or T for γ values corresponding to *cis*, *trans* and *equilibrium* molecular geometries) are calculated by the potentials corresponding to the leading configurations. For example, for the *cis* geometries of the molecule we have the system

$$
\begin{aligned}
C_<(r) &= v^0_{00}(C;r) + v^1_{10}(C;r)\, R^1_{10}(180°,90°,0°) + \\
&\quad v^2_{00}(C;r)\, R^2_{00}(180°,90°,0°) + v^2_{20}(C;r)\, R^2_{20}(180°,90°,0°) \\
C_\perp(r) &= v^0_{00}(C;r) + v^1_{10}(C;r)\, R^1_{10}(90°,90°,0°) + \\
&\quad v^2_{00}(C;r)\, R^2_{00}(90°,90°,0°) + v^2_{20}(C;r)\, R^2_{20}(90°,90°,0°) \\
C_>(r) &= v^0_{00}(C;r) + v^1_{10}(C;r)\, R^1_{10}(0°,90°,0°) + \\
&\quad v^2_{00}(C;r)\, R^2_{00}(0°,90°,0°) + v^2_{20}(C;r)\, R^2_{20}(0°,90°,0°) \\
C_\parallel(r) &= v^0_{00}(C;r) + v^1_{10}(C;r)\, R^1_{10}(\text{ind.},0°,0°) + \\
&\quad v^2_{00}(C;r)\, R^2_{00}(\text{ind.},0°,0°) + v^2_{20}(C;r)\, R^2_{20}(\text{ind.},0°,0°) \qquad (7)
\end{aligned}
$$

which can be inverted, for example, by Cramer's rule to give

$$
\begin{aligned}
v^0_{00}(C;r) &= \frac{1}{6}C_<(r) + \frac{1}{3}C_\perp(r) + \frac{1}{6}C_> + (r)\frac{1}{3}C_\parallel(r) \\
v^1_{10}(C;r) &= \frac{1}{2}C_<(r) - \frac{1}{2}C_>(r) \\
v^2_{00}(C;r) &= -\frac{1}{6}C_<(r) - \frac{1}{3}C_\perp(r) - \frac{1}{6}C_>(r) + \frac{2}{3}C_\parallel(r) \\
v^2_{20}(C;r) &= \frac{\sqrt{3}}{6}C_<(r) + \frac{\sqrt{3}}{3}C_\perp(r) + \frac{\sqrt{3}}{6}C_>(r) \qquad (8)
\end{aligned}
$$

An entirely analogous set of equations holds for the equilibrium case:

$$
\begin{aligned}
v^0_{00}(E;r) &= \frac{1}{6}E_<(r) + \frac{1}{3}E_\perp(r) + \frac{1}{6}E_>(r) + \frac{1}{3}E_\parallel(r) \\
v^1_{10}(E;r) &= \frac{1}{2}E_<(r) - \frac{1}{2}E_>(r) \\
v^2_{00}(E;r) &= -\frac{1}{6}E_<(r) - \frac{1}{3}E_\perp(r) - \frac{1}{6}E_>(r) + \frac{2}{3}E_\parallel(r) \\
v^2_{20}(E;r) &= \frac{\sqrt{3}}{6}E_<(r) + \frac{\sqrt{3}}{3}E_\perp(r) + \frac{\sqrt{3}}{6}E_>(r) \qquad (9)
\end{aligned}
$$

For the *trans* geometries, because $T_< = T_>$, the v^1_{10} term is missing:

$$
\begin{aligned}
v^0_{00}(T;r) &= \frac{1}{3}T_<(r) + \frac{1}{3}T_\perp(r) + \frac{1}{3}T_\parallel(r) \\
v^2_{00}(T;r) &= -\frac{1}{3}T_<(r) - \frac{1}{3}T_\perp(r) + \frac{2}{3}T_\parallel(r) \\
v^2_{20}(T;r) &= \frac{\sqrt{3}}{3}T_<(r) + \frac{\sqrt{3}}{3}T_\perp(r) \qquad (10)
\end{aligned}
$$

It is now convenient to define the $w_i(\gamma)$ coefficients, which establish the weight of each set of leading configurations ($i = C$, T, E) according to the corresponding γ value. Specifically, assuming the torsional potential expanded in a cosine series[24] including $\cos n\gamma$ terms ($n = 0$, 1, 2), we have, in general,

$$w_i(\gamma) = a_i + b_i \cos\gamma + c_i \cos 2\gamma$$

$i = C$, T, E. Specifically,

$$w_C(0°) = 1 \qquad w_C(180°) = 0 \qquad w_C(112.54°) = 0$$
$$w_T(0°) = 0 \qquad w_T(180°) = 1 \qquad w_T(112.54°) = 0$$
$$w_E(0°) = 0 \qquad w_E(180°) = 0 \qquad w_E(112.54°) = 1$$

allowing to compute parameters a_i, b_i, and c_i. Eventually, we have

$$w_C(\gamma) = (0.319 + 0.500 \cos\gamma + 0.181 \cos 2\gamma)$$
$$w_T(\gamma) = (0.095 - 0.500 \cos\gamma + 0.405 \cos 2\gamma)$$
$$w_E(\gamma) = (0.586 - 0.586 \cos 2\gamma) \quad (11)$$

We can now write $V_{ext}(r;\alpha,\beta,\gamma)$ in eq 2 as

$$V_{ext}(r;\alpha,\beta,\gamma) = \sum_{i=C,T,E} w_i(\gamma)[v^1_{10}(i;r)\, R^1_{10}(\alpha,\beta,0) + v^2_{00}(i;r)\, R^2_{00}(\alpha,\beta,0) + v^2_{20}(i;r)\, R^2_{20}(\alpha,\beta,0)] \quad (12)$$

where the above calculated moments 8, 9, and 10 are used, except for the $v^0_{00}(i;r)$ terms, which are employed to obtain an expression for $V_{int}(r;\alpha,\beta,\gamma)$.

Explicitly,

$$V_{int}(r,\gamma) = d(r) + e(r)\cos\gamma + f(r)\cos 2\gamma$$

where $d(r)$, $e(r)$, and $f(r)$ are obtained by imposing that the torsional potential has the value of the proper energy barrier heights for the *cis* and *trans* geometry, and the zero of the energy is taken at the equilibrium geometry. Therefore (Table 4)

$$V_{int}(r;0°) = d + e + f = 7.3623 \text{ kcal/mol}$$
$$V_{int}(r;180°) = d - e + f = 1.1036 \text{ kcal/mol}$$
$$V_{int}(r;112.54°) = d - 0.383e - 0.706f = 0 \text{ kcal/mol}$$

which can be solved to give d, e, and f. If we now want V_{int} expanded in hyperspherical harmonics with $\bar{v}^{\mu}_{MM'}$ expansion moments (see below),

$$V_{int}(r;\gamma) = \bar{v}^0_{00}(r) + \bar{v}^1_{01}(r)\, R^1_{01}(0,\pi/2,\gamma) + \bar{v}^2_{02}(r)\, R^2_{02}(0,\pi/2,\gamma)$$

We solve a 3×3 linear system, obtained from the above expression by introducing, for a given r, the values of the potential corresponding to the *cis*, *trans*, and equilibrium geometries. We finally have

$$\bar{v}^0_{00}(r) = 0.319 v^0_{00}(C;r) + 0.586 v^0_{00}(E;r) + 0.095 v^0_{00}(T;r)$$
$$\bar{v}^1_{01}(r) = 0.5 v^0_{00}(C;r) - 0.5 v^0_{00}(T;r)$$
$$\bar{v}^2_{02}(r) = 0.209 v^0_{00}(C;r) - 0.677 v^0_{00}(E;r) + 0.468 v^0_{00}(T;r) \quad (13)$$

The moment $\bar{v}^0_{00}(r)$, the coefficient of the constant R^0_{00} basis function in the intramolecular term, can be thought of as the potential averaged over the α, β angle domains and represents the isotropic part of the atom−molecule interactions, whereas $\bar{v}^1_{01}(r)$ and $\bar{v}^2_{02}(r)$ are the terms representing the anisotropies.

3. *Ab Initio* Calculations

The *ab initio* calculations for the Rg−H_2O_2 systems were performed using the Gaussian03 program.[25] The choice of the calculation level is based on the Maciel et al. studies[2] of the H_2O_2 monomer. In this work we focus on what is estimated to be an accurate calculation level, which reproduces the geometric parameters of the equilibrium geometry and gives realistic barrier heights for the *cis* and *trans* geometries, at a reasonable computational cost. The second-order Møller−Plesset level, using all electrons (MP2=FU), and the aug-cc-pVTZ basis set were chosen for He, Ne, Ar, and Kr. For Xe we have used the aug-cc-pVTZ-PP basis set according to refs 26, 27, and 28 where relativistic effects are introduced in the basis through small-core pseudopotentials. To minimize the basis set superposition error (BSSE), the full counterpoise Boys and Bernardi correction[29] was applied. Accordingly, the energies of monomers are calculated using the same full basis set, and the interaction energy is then defined as

$$E_{CP} = E_{AB}(\chi_A + \chi_B) - [E_A(\chi_A + \chi_B) + E_B(\chi_A + \chi_B)] \quad (14)$$

where χ_A and χ_B are the basis sets of each monomer of the complex AB. We calculated a set of 81 single potential energy points on the surface, for each of the eleven leading configurations, for the He−H_2O_2 and Ne−H_2O_2 systems, 92 points for the Ar−H_2O_2 and Kr−H_2O_2 and 131 points for Xe−H_2O_2. All the H_2O_2 geometry parameters are kept frozen at their equilibrium values as presented in Table 4, except γ.

The eleven different leading configurations used to explore the various features of the potential energy surfaces, four for the equilibrium geometry, four for the *cis* geometry, and three for the *trans* geometry, have been seen previously (section 1). For each system, an additional configuration to be introduced later served for assessing the accuracy of the proposed expansion. All energies were calculated as a function of r (Figure 2) between the rare gas and the center-of-mass of H_2O_2.

The analytical form of the potential energy surfaces, for each of the leading configurations, are constructed by fitting the following fifth degree generalized Rydberg function into the *ab initio* points:

$$V(R) = D_e \sum_{k=1}^{5} (1 + a_k(R - R_{eq})^k) \exp[-a_1(R - R_{eq})] + E_{ref} \quad (15)$$

where D_e, a_k, R_{eq}, and E_{ref} are adjustable parameters. A nonlinear least-squares procedure was used to obtain the values of the adjustable parameters that minimize the differences between the analytical energies obtained with the generalized Rydberg function and the MP2(FU)/aug-cc-pVTZ data. Tables are provided as Supporting Information.

4. Results and Discussion

For each of the H_2O_2−Rg systems (Rg = He, Ne, Ar, Kr, Xe), we have considered the eleven leading configurations (see Table 4) for which the atom−molecule interaction energy has been calculated at various r (the distance between the atom and the center-of-mass of the molecule) by the *ab initio* methods, explained in detail in section 3.

Figures 3−5 show both the *ab initio* energy points and the corresponding Rydberg curve fittings for the complete rare gas series and for each of the leading configurations. Further data are given as Supporting Information. The leading configurations can be distinguished into three groups, according to the geometry of the H_2O_2 molecule (*cis*, *trans*, and equilibrium) and as expected, the corresponding energy curves fall in different energy ranges: equilibrium (lower), *trans* (intermediate), *cis* (higher energies), according to the order common to all systems.

Another common trend that can be seen is that distances of minimum energy move to higher values and the well depths increase in going from lighter to heavier atoms. (A similar

TABLE 4: Geometries and Barriers for the H_2O_2 at the MP2/aug-cc-pVTZ[a] Level

molecular geometry	R_{HO} [Å]	R_{OO} [Å]	$\angle_{HOO}$ [deg]	$\angle_{HOOH}$ [deg]	barrier [kcal mol^{-1}]
equilibrium	0.9668	1.4537	99.6128	112.5422	0
	(0.950 ± 0.005)[b]	(1.475 ± 0.004)[b]	(94.8 ± 2)[b]	(119.8 ± 3)[b]	
	(0.9627)[c]	(1.4525)[c]	(99.91)[c]	(112.46)[c]	
cis	0.9670	1.4628	104.1053	0.0000	7.3623
	(0.9628)[c]	(1.4630)[c]	(104.14)[c]	(0.0)[c]	(7.276)[c]
					(7.033 ± 0.071)[d]
trans	0.9663	1.4652	97.9109	180.0000	1.1036
	(0.9616)[c]	(1.4637)[c]	(98.31)[c]	(180.0)[c]	(1.078)[c]
					(1.104 ± 0.011)[d]

[a] Theoretical data from ref 2. [b] Experimental data from ref 30. [c] Theoretical data from ref 31 at the CCSD(T)/cc-pVQZ level. [d] Experimental data from ref 24.

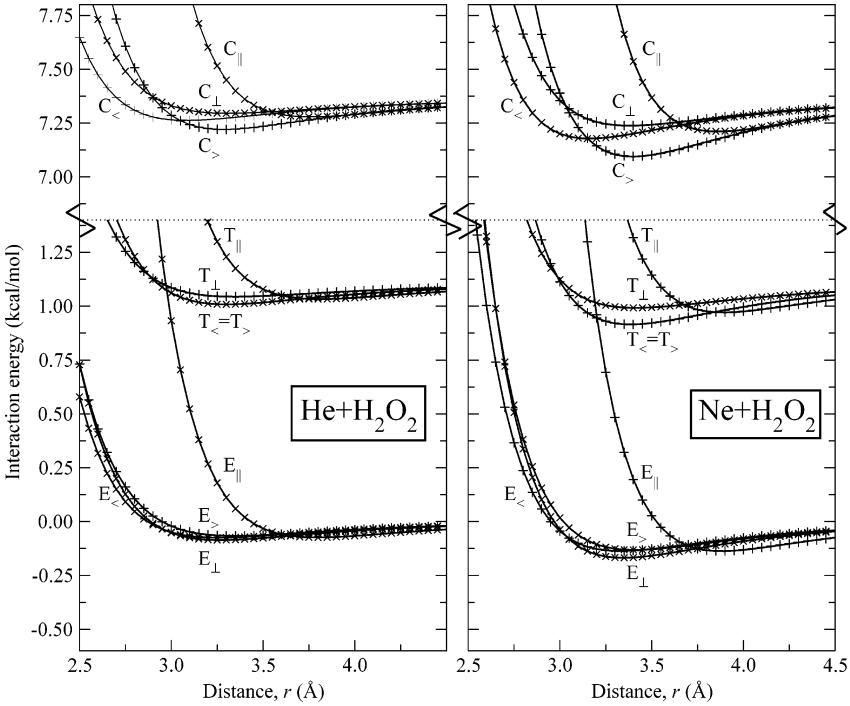

Figure 3. $He-H_2O_2$ and $Ne-H_2O_2$ interaction energies for the leading configurations of Table 3 as a function of the distance of the rare gas from the center-of-mass of the hydrogen peroxide molecule. Crosses indicate *ab initio* points (others lie outside of the drawings) and curves are from Rydberg fits, as described in the text.

behavior was also observed in previous studies of H_2O[10] and H_2S-Rg systems.[11])

It is worth noting that the "perpendicular" approach ($\beta = 90°$, $\alpha = 90°$), whatever the geometry of the molecule ($E_\perp$, $C_\perp$, and $T_\perp$), leads to systematically more stable systems than the corresponding "collinear" approaches ($\beta = 0°$), $E_{||}$, $C_{||}$, and $T_{||}$, which are also much more repulsive. Among the *cis* configurations (see Figure 1), the one at $\beta = 90°$ and $\alpha = 180°$, ($C_>$) with the atom lying on the molecule plane and approaching the molecule from the hydrogen atom side, results to be the most stable, for all the rare gas series. The difference in energy between these curves and the $C_<$ curves, with the atom at the opposite side of the hydrogens, increases from He to Xe. The $C_<$ curve exhibits the softest potential profiles.

Concerning the *trans* configurations the two directions $\alpha = 0°$ and $\alpha = 180°$ are equivalent and the $T_<$ and $T_>$ curves coincide, being the ones with the lowest energy minimum.

The equilibrium configurations are those with the lowest energy profiles. Among them, the $E_\perp$ configuration is the most stable (the lowest energy minimum) and at small distances is more repulsive than both $E_>$ and $E_<$ curves.

The energy profiles corresponding to $\beta = 0°$ configurations, with the atom coming along the O−O bond direction, are shifted at longer distances systematically for all the rare gas series. This can be explained by the fact that for the same value of the distance from the center-of-mass of the molecule, the atom can get closer to an oxygen atom when coming along the O−O bond directions, than if coming from directions perpendicular to the bond.

Figure 6 shows a comparison of the *ab initio* energy profiles for all the rare gas series, corresponding to the molecule at the equilibrium ($\gamma = 112.54°$) and $\alpha = 56.27°$ and $\beta = 90°$ with the analogous curves as obtained from the hyperspherical expansion. This configuration was not included in the calculation of the expansion moments and the comparison is a useful test for the validity of the hyperspherical expansion. Although the difference can be appreciable in the well depths, especially for the heavier atoms, there is a substantially good agreement (very good for Helium and Neon), concerning the minimum energy distances and the shape of the curves, a remarkable fact, considering that the configuration is far from those included in the calculation of the hyperspherical expansion.

Figure 7 shows the expansion moments for the $Ar-H_2O_2$ interaction, as a function of the distance from the molecule center of mass. The isotropic part of the potential, referred to

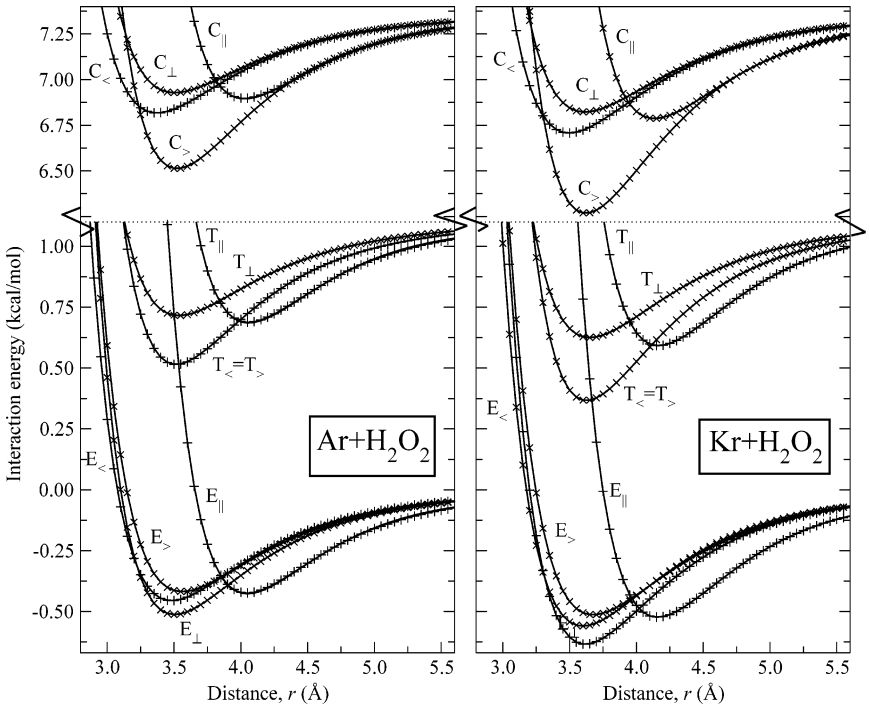

Figure 4. $Ar-H_2O_2$ and $Kr-H_2O_2$ interaction energies for the leading configurations of Table 3 as a function of the distance of the rare gas from the center-of-mass of the hydrogen peroxide molecule. Crosses indicate *ab initio* points (others lie outside of the drawings) and curves are from Rydberg fits, as described in the text.

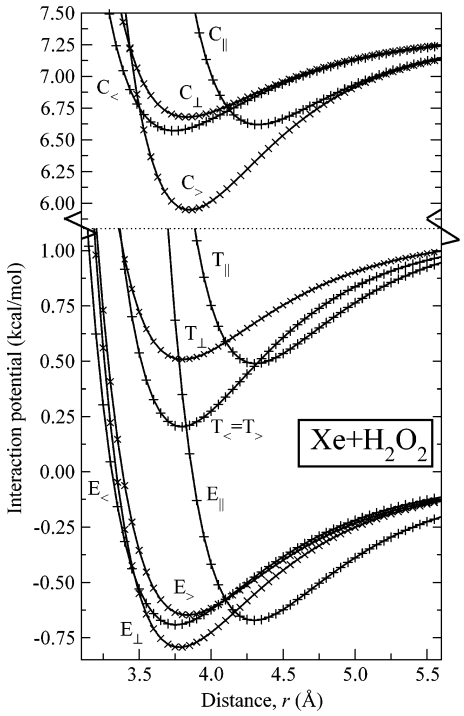

Figure 5. $Xe-H_2O_2$ interaction energies for the leading configurations of Table 3 as a function of the distance of the rare gas from the center-of-mass of the hydrogen peroxide molecule. Crosses indicate *ab initio* points (others lie outside of the drawing) and curves are from Rydberg fits, as described in the text.

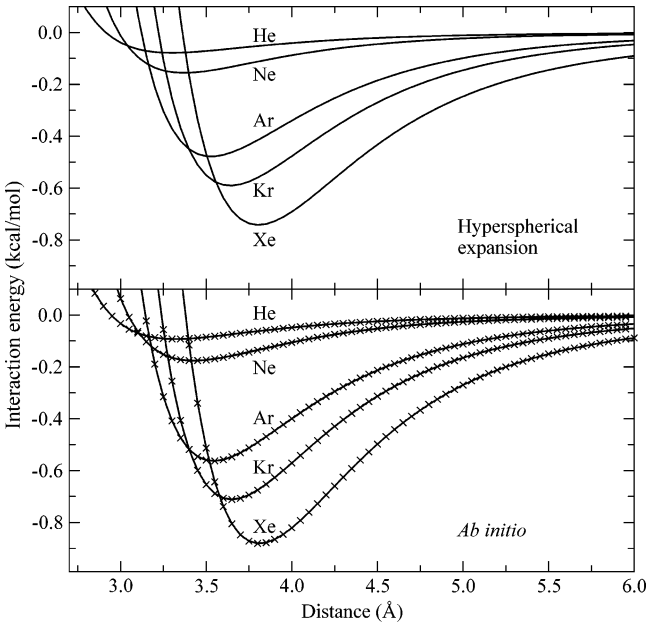

Figure 6. Rare gas$-H_2O_2$ interaction energies as a function of the distance of the rare gas from the center-of-mass of the hydrogen peroxide molecule, for the equilibrium ($\gamma = 112.54°$) geometry and the rare gas atom approaching from a direction given by $\beta = 90°$ and $\alpha = 56.27°$. Lower panel: crosses indicate *ab initio* points (others lie outside of the drawing) and curves are from Rydberg fits, as described in the text. Upper panel: curves indicate hyperspherical expansion as described in the text.

the *cis*, *trans*, and equilibrium geometry of H_2O_2, is plotted along with its value averaged over the same three molecular geometries, using the *w* coefficients of section 2.3. Also the contribution of the anisotropy is shown by the moments $\bar{v}^1_{01}$ and $\bar{v}^2_{02}$. These are nearly constant in most of the considered distance range and do not have a minimum. As expected, the isotropic terms of the potential show minima and for $r \rightarrow \infty$ asymptotically tend to the energy of the isolated H_2O_2 molecule in the *cis*, *trans* and equilibrium configurations.

The quantity in Figure 7, which allows comparison with other systems, is $\bar{v}^0_{00}(r)$, representing the isotropic component of the interaction, corresponding to full averaging over both internal torsional angle γ and the external angles α and β. Table 5 lists well depths and positions for this term, which is the one that shows the possibility of being measurable in molecular beam

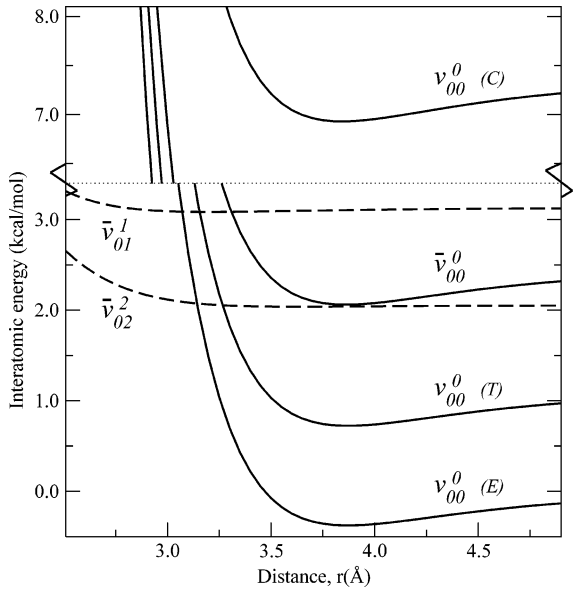

Figure 7. Dependence on atom−molecule distance of some representative isotropic (continuous curves) and anisotropic (dashed curves) moments of the hyperspherical expansion for Ar−H_2O_2.

TABLE 5: Well Depth, ϵ (in kcal/mol), and Corresponding Atom−Molecule Distance, r_m, of the Avarage Isotropic Expansion Moment $\bar{v}_{00}^0$

system	r_m	ϵ
He−H_2O_2	3.626	0.0660
Ne−H_2O_2	3.734	0.1234
Ar−H_2O_2	3.870	0.3944
Kr−H_2O_2	3.967	0.4951
Xe−H_2O_2	4.106	0.6419

scattering experiments. It is interesting to compare the values in Table 5 with those of the recently investigated systems, H_2O[10] and H_2S[11] with the rare gases. The series of r_m values for the H_2O_2 systems investigated here is found to be intermediate between the corresponding values for H_2O and H_2S, in agreement with what is expected from known correlations of van der Waals forces with the corresponding atomic and molecular polarizabilities of the interacting parameters.[12] Well depths follow similar trends, although less quantitatively.

Regarding anisotropies, as can be seen from Figures 3−5, they follow the same trends for all systems, and Figure 7 confirms that they are generally small and slowing varying. This can be visualized in Figure 8 (where dependence on the torsional angle γ is shown, properly freezing the angles α and β) and in Figure 9 (where dependence on the α angle is shown, at fixed $\beta = 90°$ and $\gamma = 112.54°$). These graphs have been obtained by using the full potential energy surface generated by the hyperspherical harmonics expansion, which produce a smooth interpolation among the curves corresponding to the 12 leading configurations that we have considered in this paper.

5. Concluding Remarks and Perspectives

The interaction potentials of H_2O_2 with the five rare gases has been studied by *ab initio* calculations and represented through a hyperspherical harmonic expansion suited for atom−floppy molecule interactions, floppiness in this case being due to the torsion mode around the O−O bond.

To determine the expansion moments, we chose a dozen significant (leading) configurations, thought to be representative also on account of the symmetries of the systems. This has allowed us to build up an interaction potential expansion

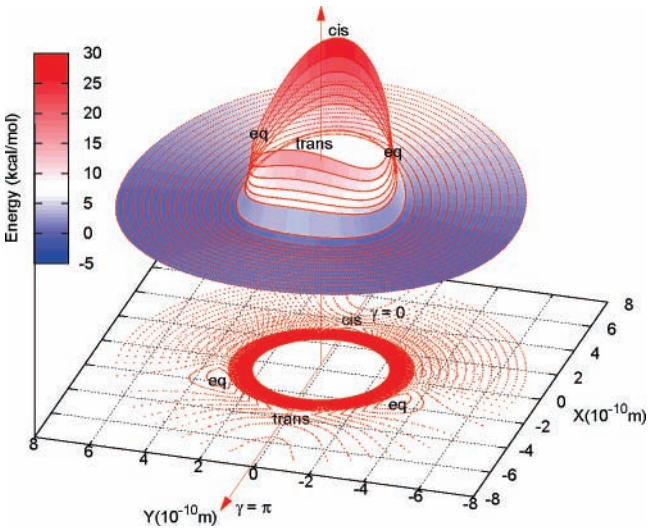

Figure 8. Illustration of the potential energy surface for the interaction of Ar with H_2O_2, as the torsional angle varies in the *xy* plane (see Figure 1). The radial coordinate in this plane is the distance *r* of the Ar atom from the center-of-mass of the H_2O_2 molecule, and the approach is perpendicular to the O−O bond in the direction having $\alpha = 0°$ and $\beta = 90°$. Visible are ridges corresponding to *trans* and *cis* barriers separating the valleys where the two enantiomeric equilibrium geometries lie. The other rare gases behave similarly.

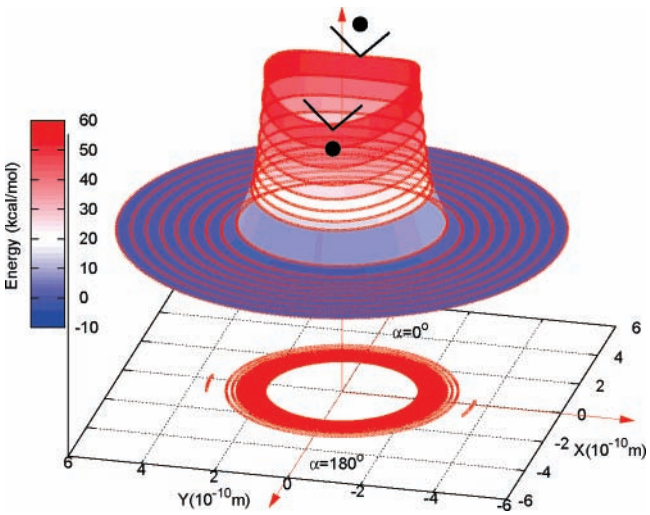

Figure 9. View of the potential energy surface for the interaction of Ar with H_2O_2, as the angle α varies in the *xy* plane (see Figures 1 and 2) in the equilibrium geometry ($\gamma = 112.54°$). The direction of approach is given by the angle $\beta = 0°$ and therefore takes place in the *xy* plane, perpendicular to the spine of the book. The radial coordinate in this plane is the distance *r* of the Ar atom from the center-of-mass of the H_2O_2 molecule, and the variation with the angle α shows that the potential energy surface is pratically isotropic from this perspective; barely visible are valley bottoms arising from evolutions of minima when the spine of the book is hit from outside or inside.

potentially useful for dynamical studies by classical or quantum mechanics. For early investigations by classical trajectories of clustering of H_2O_2 molecule by Ar, see refs 32 and 33. This work provides a formulation that is particularly suited for future quantum mechanical calculations, specifically of chirality changing collisions.

The hyperspherical expansion appears to be a powerful tool: it allows implementation of symmetries and of further information coming from introduction of additional configurations. Interpretation of experimental molecular beam scattering studies can also be assisted by these investigations. However, production of intense and stable beams of H_2O_2 still appears to be a

challenge, although it would be extremely useful to extend the phenomenology being established for interactions of similar molecules of remarkable relevance, H_2O[10] and H_2S.[11] At this stage, we can observe that one of the present results—the $v_{00}^0(r)$ term that comes out of averaging over both the intramolecular torsional angle γ and intermolecular orientational angles α and β—permits a favorable comparison with the H_2O and H_2S cases, being the average well depths and ranges of the correct magnitudes, as expected from currently available estimates for typical van der Waals interactions as reviewed in ref 12. The delicate question of the role of the hydrogen bonding[10] in these complexes, and more generally in those involving peroxides, has not been specifically addressed in this work but should be possibly revisited when further inputs come from experiments.

Acknowledgment. Work in Perugia is supported by MIUR (the Italian Ministero per l'Universitá e la Ricerca), through PRIN (Progetti di Ricerca di Interesse Nazionale) and FIRB (Fondo per la Ricerca di Base) contracts, and by ASI (Agenzia Spaziale Italiana).

Supporting Information Available: *Ab initio* data on configurations of the $Rg-H_2O_2$ systems, comparison between *ab initio* calculations and real hyperspherical harmonics expansion and on the parameters for the Rydberg fits. This material is available free of charge via the Internet at http://pubs.acs.org.

References and Notes

(1) Maciel, G. S.; Cappelletti, D.; Pirani, F.; Aquilanti, V. *Adv. Quantum Chem.*, in press.

(2) Maciel, G. S.; Bitencourt, A. C. P.; Ragni, M.; Aquilanti, V. *Chem. Phys. Lett.* **2006**, *432*, 383.

(3) Maciel, G. S.; Bitencourt, A. C. P.; Ragni, M.; Aquilanti, V. *Int. J. Quantum Chem.* **2007**, *107*, 2697.

(4) Maciel, G. S.; Bitencourt, A. C. P.; Ragni, M.; Aquilanti, V. *J. Phys. Chem. B*, in press.

(5) Maciel, G. S.; Aquilanti, V. Manuscript in preparation.

(6) Daza, M. C.; Dobado, J. A.; Molina, J. M.; Salvador, P.; Duran, M.; Villaveces, J. L. *J. Chem. Phys.* **1999**, *110*, 11806.

(7) Daza, M. C.; Dobado, J. A.; Molina, J. M.; Villaveces, J. L. *Phys. Chem. Chem. Phys.* **2000**, *2*, 4094.

(8) Molina, J. M.; Dobado, J. A.; Daza, M. C.; Villaveces, J. L. *J. Mol. Structure (THEOCHEM)* **2002**, *580*, 117.

(9) Elange, M.; Parthasarathi, R.; Subramanian, V.; Ramachandran, C. N.; Sathyamurthy, N. *J. Phys. Chem. A* **2006**, *110*, 6294.

(10) Aquilanti, V.; Cornicchi, E.; Teixidor, M. M.; Saendig, N.; Pirani, F.; Cappelletti, D. *Angew. Chem. Int. Ed.* **2005**, *44*, 2356.

(11) Cappelletti, D.; Vilela, A. F. A.; Barreto, P. R. P.; Gargano, R.; Pirani, F.; Aquilanti, V. *J. Chem. Phys.* **2006**, *1*, 125.

(12) Pirani, F.; Maciel, G. S.; Cappelletti, D;, Aquilanti, V. *Int. Rev. Phys. Chem.* **2006**, *25*, 165.

(13) Aquilanti, V.; Ascenzi, D.; Cappelletti, D.; Pirani, F. *J. Chem. Phys.* **1995**, *99*, 13620.

(14) Pirani, F.; Bartolomei, M.; Aquilanti, V.; Cappelletti, D.; Scotoni, M.; Vescovi, M.; Ascenzi, D.; Bassi, D.; Cappelletti, D. *J. Chem. Phys.* **2003**, *119*, 265.

(15) Cappelletti, D.; Bartolomei, M.; Aquilanti, V.; Pirani, F.; Demarchi, G.; Bassi, D.; Iannotta, S.; Scotoni, M. *Chem. Phys. Lett.* **2006**, *42*, 420.

(16) Aquilanti, V.; Maciel, G. S. *Orig. Life Evol. Biosph.* **2006**, *36*, 435.

(17) Lee, H. N.; Su, T. M.; Chao, I. *J. Phys. Chem. A* **2004**, 108, 2567; unpublished work. We thank Professor Su for informative correspondence.

(18) Aquilanti, V.; Cavalli, S.; Grossi, G. *J. Chem. Phys.* **1986**, *85*, 1362.

(19) Aquilanti, V.; Cavalli, S.; Coletti, C.; Di Domenico, D.; Grossi, G. *Int. Rev. Phys. Chem.* **2001**, *20*, 673.

(20) Varshalovich, D. A.; Moskalev, A. N.; Khersonskii, V. K. *Quantum Theory of Angular Momentum*; World Scientific: Singapore, 1988.

(21) Aquilanti, V.; Cavalli, S. *J. Chem. Phys.* **1985**, *85*, 1355.

(22) Ragni, M.; Bitencourt, A. C. P.; Aquilanti, V. *Int. J. Quantum Chem.* **2007**, *107*, 2870.

(23) Wigner, E. P. *Group Theory and its Applications to the Quantum Theory of Atomic Spectra*; Academic Press Inc.: New York, 1959.

(24) Hunt, R. H.; Leacock, R. A.; Peters, C. W.; Hecht, K. T. *J. Chem. Phys.* **1965**, *42*, 1931.

(25) Frisch, M. J.; Trucks, G. W.; Schlegel, H. B.; Scuseria, G. E.; Robb, M. A.; Cheeseman, J. R.; Montgomery, J. A., Jr.; Vreven, T.; Kudin, K. N.; Burant, J. C.; Millam, J. M.; Iyengar, S. S.; Tomasi, J.; Barone, V.; Mennucci, B.; Cossi, M.; Scalmani, G.; Rega, N.; Petersson, G. A.; Nakatsuji, H.; Hada, M.; Ehara, M.; Toyota, K.; Fukuda, R.; Hasegawa, J.; Ishida, M.; Nakajima, T.; Honda, Y.; Kitao, O.; Nakai, H.; Klene, M.; Li, X.; Knox, J. E.; Hratchian, H. P.; Cross, J. B.; Bakken, V; Adamo, C.; Jaramillo, J.; Gomperts, R.; Stratmann, R. E.; Yazyev, O.; Austin, A. J.; Cammi, R.; Pomelli, C.; Ochterski, J. W.; Ayala, P. Y.; Morokuma, K.; Voth, G. A.; Salvador, P.; Dannenberg, J. J.; Zakrzewski, V. G.; Dapprich, S.; Daniels, A. D.; Strain, M. C.; Farkas, O.; Malick, D. K.; Rabuck, A. D.; Raghavachari, K.; Foresman, J. B.; Ortiz, J. V.; Cui, Q.; Baboul, A. G.; Clifford, S.; Cioslowski, J.; Stefanov, B. B.; Liu, G.; Liashenko, A.; Piskorz, P.; Komaromi, I; Martin, R. L.; Fox, D. J.; Keith, T.; Al-Laham, M. A.; Peng, C. Y.; Nanayakkara, A.; Challacombe, M.; Gill, P. M. W.; Johnson, B.; Chen, W.; Wong, M. W.; Gonzalez, C.; Pople J. A. *Gaussian 03*, revision C.02; Technical report; Gaussian, Inc.: Wallingford, CT, 2004.

(26) Alexander, W. A.; Troya D. *J. Phys. Chem. A* **2006**, *110*, 10834.

(27) Peterson, K. A.; Figgen, D.; Goll, E.; Stoll, H.; Dolg, M. *J. Chem. Phys.* **2003**, *119*, 11113.

(28) Basis sets were obtained from the Extensible Computational Chemistry Environment Basis Set Database, Version 02/02/06, as developed and distributed by the Molecular Science Computing Facility, Environmental and Molecular Sciences Laboratory, which is part of the Pacific Northwest Laboratory, P.O. Box 999, Richland, Washington 99352, U.S.A., and funded by the U.S. Department of Energy. The Pacific Northwest Laboratory is a multiprogram laboratory operated by Battelle Memorial Institute for the U.S. Department of Energy under contract DE-AC06-76RLO 1830.

(29) Boys, S. F.; Bernardi, F. *Mol. Phys.* **1970**, *19*, 553; **2002**, *19*, 65.

(30) Redington, R. L.; Olson, W. B.; Cross, P. C. *J. Chem. Phys.* **1962**, *36*, 1311.

(31) Koput, J. *Chem. Phys. Lett.* **1965**, *236*, 516.

(32) Finney, L. M.; Martens, C. C. *J. Phys. Chem.* **1992**, *96*, 10256.

(33) Finney, L. M.; Martens, C. C. *J. Phys. Chem.* **1993**, *97*, 13477.